Measurements and Analysis of Photochemical Oxidants and Trace Gases in the Rural Troposphere of the Southeast United States

VINEY P. ANEJA,* MITA DAS, DEUG-SOO KIM, AND BENJAMIN E. HARTSELL
Department of Marine, Earth and Atmospheric Sciences,
North Carolina State University, Raleigh, North Carolina 27695-8208, USA

(Received 18 April 1994 and in revised form 26 October 1994)

Abstract. Ambient concentrations of photochemical oxidants (O_3, PAN, HNO_3, H_2O_2) and various trace species including reactive nitrogen compounds as well as total NO_y were measured during June and early July 1992 at a rural site, SONIA, in the central Piedmont region of North Carolina, as a part of the Southern Oxidants Study. The measurements were made in an effort to provide a comprehensive understanding of tropospheric photochemistry in the rural Southeastern United States. NO_y, NO_2, and NO showed diurnal variations with maxima in the morning between 0600 and 0900 EST. The maximum NO_y, NO, and NO_2 concentrations reached were 14.5, 5.4, and 7.8 ppbv, respectively. The mean NO_y concentration was found to be 2.63 ± 1.72 ppbv ($n = 819$) with an average daily maximum of 3.6 ppbv. The mean concentrations of NO and NO_2 for the entire period of measurement were found to be 0.18 ± 0.37 ppbv ($n = 794$) and 1.31 ± 0.99 ppbv/($n = 769$). H_2O_2, HNO_3, and PAN showed diurnal variation with maxima in the afternoon and minima at night. Mean concentrations were found to be 0.52 ± 0.36 ppbv ($n = 312$), 0.67 ± 0.33 ppbv ($n = 250$), and 0.41 ± 0.24 ppbv ($n = 578$). The NO_x/NO_y ratio was used as an indicator of the chemical age of airmasses and the ratio showed strong positive correlations with the photochemical oxidants HNO_3 ($r = 0.76$), PAN ($r = 0.68$), and O_3 ($r = 0.79$) measured at the site. The relationship between the accumulation rate of O_3 and the deviation from the photostationary state was examined based on the measured PSS constant obtained from the values of [O_3], [NO], and [NO_2] measured at the site.

INTRODUCTION

Photochemical oxidants comprise a class of highly reactive chemical compounds produced within the Earth's atmosphere. In the upper atmosphere, ozone, the most abundant photochemical oxidant, protects life from the harmful effects of ultraviolet light from the sun. Paradoxically, near the Earth's surface ozone and other photochemical oxidants can, at sufficient concentrations, have adverse effects on human, plant, and animal life.

Most major metropolitan areas in the United States exhibit peak summertime concentrations of ozone above the National Ambient Air Quality Standard (NAAQS), established by the Environmental Protection Agency (EPA) for the protection of human health.[1] More than a decade has elapsed since implementation of the current air quality standard. In that time, ozone has proven to be one of the most pervasive and difficult to control of the major air pollutants in this country.[2] Much of this difficulty can be traced to the nature of photochemical oxidants themselves. Unlike most other air pollutants, such as sulfur dioxide, which are emitted directly into the atmosphere, ozone and other photochemical oxidants are formed within the atmosphere by a complex set of chemical reactions involving Volatile Organic Compounds (VOCs), nitrogen oxides (NO_x) and sunlight. Major reactions leading to the formation of ozone, peroxyacetyl nitrate (PAN), HNO_3, and H_2O_2 are given in Table 1.

The photochemical precursors of ozone are the oxides of nitrogen (NO_x), carbon monoxide (CO), methane (CH_4), and nonmethane hydrocarbons (NMHCs). Due to high reactivity and relatively large sources, NO_x and NMHC represent the most important

*Author to whom correspondence should be addressed.

ozone precursors in most areas of the United States. Reactions r1 and r2 in Table 1 represent the only formation process of ozone in the troposphere. Ozone formation is driven by the cycle of odd hydrogen (=OH+HO_2+RO_2 radicals) reactions that are responsible for the oxidation of NMHCs to their byproducts. The odd hydrogen cycle is important because the rates of ozone-forming reactions are governed by the availability of OH. NO_x plays a critical role in reactions with CO, CH_4, and nonmethane hydrocarbons (NMHCs) that determine the distribution of ozone (O_3) and hydroxyl radical (OH), and the interconversion between OH and hydroperoxyl radical (HO_2). An understanding of this distribution is important because OH and HO_2 radicals regulate the rates of destruction of long-lived species and determine the rates of transformation of many reactive species to reservoir species, thus changing their susceptibility to removal processes and long-range transport.[3a,b]

In the lower atmosphere, oxides of nitrogen are emitted primarily from anthropogenic processes such as combustion of fossil fuels and biomass burning.[4] In rural/remote areas, however, natural processes that exhibit spatial and temporal variability, such as soil emission of oxides of nitrogen, may be significant sources of atmospheric NO_x.[5–9] Anthropogenic sources are generally confined to small geographic areas and can be well defined. On the other hand, natural sources of NO_x are more widespread and less intense, making quantitative estimation much more difficult.[10]

The oxides of nitrogen are also oxidized in the atmosphere. The compounds enter the atmosphere from a variety of natural and anthropogenic sources, largely as nitric oxide. The rapid daytime interconversion of NO and NO_2 that involves the peroxy radical, RO_2, is the photochemical mechanism for the formation of ozone, as described above. NO and NO_2 are subsequently converted to a variety of other organic and inorganic nitrates. The entire family of compounds is generally referred to as the reactive nitrogen oxides, and the sum of the concentrations of all the compounds that comprise the family is referred to as NO_y. The more oxidized forms are less chemically active in the atmosphere than are NO and NO_2. The organic nitrates serve to sequester NO_x, and provide a means to transport NO_y from source regions to more remote parts of the atmosphere. The nitrates are eventually converted into nitric acid. The deposition of nitric acid and the nitrate ion is the chief removal mechanism for the nitrates from the atmosphere. Interconversion of NO_x into other odd-nitrogen species, therefore, can be an effective mechanism for the long-range transport of reactive oxidized nitrogen to remote regions.[11,12]

In the rural southeastern US, summertime midday O_3 concentrations of 50–70 ppb are common.[13–15] In many ways, the South, and the Southeast in particular, represents a natural laboratory for the study of oxidant formation. The same mix of sunlight, moisture, and high temperatures that makes the South's forests and agriculture highly productive also contributes to high oxidant formation rates. Further, the relatively low population density and level of industrialization in the region may make natural sources of ozone precursors potentially important. Vegetation, including crops, forests, and ornamental plants, is known to produce VOCs as part of natural respiratory, photosynthetic, and stress defense mechanisms. Emission rates of these VOCs typically increase with temperature and/or photosynthetic rates that are, on average, higher in the South than in more northerly locations. These emission rates, in combination with a generally dense vegetative cover, make natural VOC emissions particularly high in the southern US. The Southern Oxidants Study (SOS) was initiated in response to this problem (University Corporation for Atmospheric Research (UCAR), 1990).

Table 1. Major chemical reactions involving nitrogen species leading to the formation of O_3, PAN, and H_2O_2 in the atmosphere

Photostationary state (NO, NO_2, and O_3):

$$NO_2 + h\nu\ (\lambda \leq 420\ \text{nm}) \longrightarrow NO + O\ (^3P) \quad \text{(r1)}$$

$$O_2 + O\ (^3P) \xrightarrow{M} O_3 \quad \text{(r2)}$$

$$NO + O_3 \longrightarrow NO_2 + O_2 \quad \text{(r3)}$$

Peroxy radical disruption of photostationary state:

$$NO + HO_2\cdot \longrightarrow NO_2 + OH\cdot \quad \text{(r4)}$$

$$NO + RO_2\cdot \longrightarrow NO_2 + RO\cdot \quad \text{(r5)}$$

Formation of HNO_3 (during day):

$$NO_2 + OH\cdot \xrightarrow{M} HNO_3 \quad \text{(r6)}$$

Formation and thermal decomposition of PAN, and loss of PAN with NO:

$$CH_3CO_3 + NO_2 \longleftrightarrow CH_3CO_3NO_2 \quad \text{(r7)}$$

$$CH_3CO_3 + NO \longrightarrow CH_3 + CO_2 + NO_2 \quad \text{(r8)}$$

Formation of H_2O_2:

$$NO_2 + OH\cdot \xrightarrow{M} HO_2\cdot + HO_2\cdot$$

$$\xrightarrow{H_2O,\,M} H_2O_2 + O_2 \quad \text{(r9)}$$

The meteorology of the South, and the Southeast in particular, is conducive to the generation of high concentrations of photochemical oxidants. During the summer and early fall, stagnant high pressure systems often develop over the southeast. The mostly clear skies and low winds associated with these systems allow a steady buildup of contaminants, including ozone precursors, and are ideal for the production of oxidants. During pollution episodes, O_3 levels in excess of the 120 ppb NAAQS have been measured at rural sites.[1-14]

This paper reports the observations and analysis of photochemical oxidants (O_3, H_2O_2, HNO_3, and PAN) and other trace gases, and discusses tropospheric photochemistry at a rural SOS site, SONIA (Southeastern Oxidant and Nitrogen Intensive Analysis) in the Southeastern United States. Because site SONIA is indicative of a typical rural setting throughout much of the Southeast United States, it is hoped that the analysis and discussion of the measurements made at site SONIA may shed light on the regional distribution of the oxidants and their precursor species (NMHCs and NO_x) in this region.

EXPERIMENTAL

In rural and remote areas, a quantitative knowledge of the distribution of oxidants and oxidant precursor species is critical to the understanding of regional tropospheric photochemistry, and to the development and analysis of global and regional atmospheric models. For this reason, a multi-year study of oxidant and nitrogen chemistry is being conducted in the Southeast United States as part of the Southern Oxidants Study funded by the United States Environmental Protection Agency (US EPA). As part of this study, the Air Quality group at North Carolina State University in Raleigh, NC operated an enhanced chemistry site, site SONIA (Fig. 1) near the town of Candor, NC, in the central Piedmont region of North Carolina (35.26 °N, 79.84 °W, ~170 m MSL). From 6 June 1992 to 7 July 1992 an intensive measurement period was operated where NO, NO_2, NO_y, PAN, H_2O_2, HNO_3, and speciated NMHCs were also monitored. Measurements of O_3, particulates, and meteorological data are measured year round at the National Dry Deposition Network (NDDN) site. The sampling site is in an open field (area ~1200 m^2) which was previously used to grow soybeans (~10 years prior to this study), and is surrounded by mixed deciduous and coniferous forest. The site is located on the eastern border of the Uwharrie National Forest. Four large urban areas of North Carolina are within a 150-km radius of the sampling site. Three sources of anthropogenic pollution, Raleigh–Durham, Greensboro, and Winston-Salem as well as the junction between two busy interstate highways, I-40 and I-85, are situated to the north and northeast of the site (Fig. 1).

Ambient air was drawn from a height of 10 m through a 7.62-cm (3-inch) I.D. glass sampling tower by a 3.115×10^4 L/min (1100-cfm) blower in order to limit sample residence time. The residence time to the base of the tower was calculated to be ~0.25 s. A 16-port glass manifold was installed at the base of the glass sampling tower above the blower to permit sampling access. All species, with the exception of total NO_y, HNO_3, and particulate NO_3^-, were sampled from the manifold via 5-m lengths of 0.635-cm (1/4 ") O.D. Teflon tubing. To maximize the efficiency of NO_y conversion for its measurement, a heated (325 °C) molybdenum converter was mounted at the top, adjacent to the 10-m tower. The NO_y sample, converted to NO and less susceptible to loss in the sampling line, was transferred to the high-sensitivity NO monitor by a 10-m, 0.635-cm (1/4") Teflon tube.

Ambient NO and NO_y were measured with a single instrument, the TECO 42S (Thermo Environmental Instruments Inc.) chemiluminescent high sensitivity analyzer. This instrument utilizes the reaction between NO and reagent O_3 which produces a chemiluminescence detected by a photomultiplier tube. The analyzer has an internal molybdenum converter heated to ~325 °C. It converts NO_y species to NO. The results of extensive tests of this conversion technique, both in the laboratory and field measurements, have been reported. The conversion efficiency of NO_2, HNO_3, N_2O_5, and PAN have all been found to be near 100% with this technique, while N_2O, N_2, and NH_3 are not converted to any

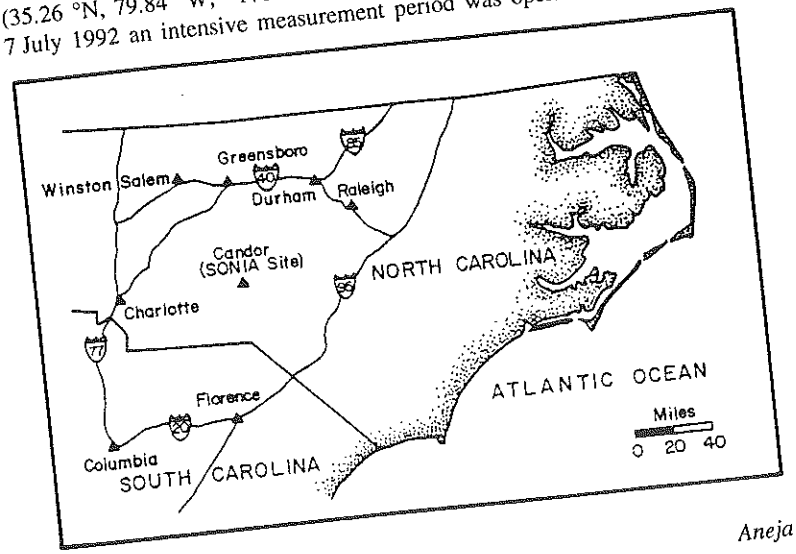

Fig. 1. Map of sampling site SONIA near Candor, North Carolina.

appreciable degree.[16,17] For this experiment, as mentioned above, a second heated molybdenum converter was mounted at the top of the 10-m tower, and all calibrations were made through both converters. For the laboratory operating conditions, the instrument detection limit is 50 parts per trillion volume (pptv) for both NO and NO_y.

HNO_3 and particulate nitrate (NO_3^-) were measured using the filter pack method. The filter pack was placed at 10 m, and the air was drawn through it by a vacuum pump on the ground connected to the filter pack by 1/4" Teflon tubing. Sampling air flow rate was maintained at 24 L/min, and was checked each time new filters were installed in the filter pack. A 5-μm Teflon filter was used to collect the particulate nitrate, and a 5-μm nylon filter was used to collect gaseous HNO_3. The collected filters were later desorbed into a buffer solution, and the solution was analyzed with an ion chromatograph to determine the nitrate content. The detection limits for both HNO_3 and NO_3^- are ~30 pptv.

Ambient NO_2 was measured directly with the LMA-3 luminol-based NO_2 analyzer from Scintrex Ltd. The LMA-3 Luminox monitor operates by detecting the chemiluminescence produced when NO_2 encounters a surface wetted with a specially formulated luminol solution. The monitor does not require prior conversion of NO_2 to NO as do other chemiluminescence detectors. The luminol solution is oxidized producing chemiluminescence (<425 nm), and a photomultiplier tube (PMT) detects the intensity of the light. The signal from the PMT is directly proportional to the concentration of NO_2 in the air. Under laboratory conditions the detection limit of the instrument is ~5 pptv, calculated as the noise equivalent of a clean air sample.[18] Interference of PAN and O_3 with the instrument are ~20% and 1%, respectively. An O_3 scrubber was installed which scrubs 99.5% of O_3 at 50 ppbv to reduce the O_3 interference. PAN interference was resolved by measurement of PAN.

PAN was monitored with a specially constructed packed-column gas chromatograph which employed a Valco Instruments electron capture detector Model 140-BN to detect the PAN peak. The GC column was a 60-cm long by 1/8" O.D. nickel tubing packed with 10% Carbowax 600 supported by 60/80 mesh acid-washed substrate. Retention time for the PAN peak was 2 min and 40 s, or 45% of the retention time of the water vapor peak. The GC used a UHP P-5 mix (5% Methane–95% Argon) as a carrier gas, and the electron capture detector developed a stable standing current of 4.5×10^{-8} A at an attenuation of 2^4 A 5-ml volume of ambient air was injected onto the column every 15 min, giving four data points per hour.

Ambient gas-phase hydrogen peroxide was measured using a continuous dual channel fluorometric analyzer based on the horseradish peroxidase method.[19] The analyzer measures total peroxides on one channel, and, by specific enzymatic destruction of hydrogen peroxide, only organic peroxides on the other channel. Hydrogen peroxide is then obtained as the difference between the total and organic peroxides. Gas-phase total and organic peroxides were recorded on a chart recorder and extracted manually as 12-min averages. The data was then consolidated into hourly averages.

All of the instruments were calibrated according to Southern Oxidants Study QA/QC protocol.[20]

RESULTS AND DISCUSSION

Diurnal Variations of O_3, PAN, and H_2O_2

Figure 2 is a time-series plot of O_3, PAN, and H_2O_2 from June 23 to June 28, 1992. All three photochemical oxidants show similar diurnal profiles with morning minima and afternoon maxima, in accordance with expected photochemical production of the three species. Typically, maximum ozone concentrations were observed between 1400–1600 Eastern Standard Time (EST), and minimum concentrations, between 0500–0700 EST. PAN minimum concentration occurred at ~0500 EST followed by a steady increase to about 1200 EST, exhibiting a broad maximum between 1200–1500 EST. H_2O_2 formation, however, was found to lag behind both PAN and O_3 formation in the photooxidation process. The continued increase in the concentrations of these species into the afternoon is thought to be evidence of their photochemical production from either locally-generated or -transported precursor species. The gradual decrease of these photochemical oxidants into the late evening is observed as production is overtaken by loss processes such as enhanced dry deposition under the subsiding boundary layer.

The daily trends of PAN and O_3 concentration appear to be generally similar except for the early morning rise in PAN which is attributed to downward mixing of undepleted air from above the nocturnal boundary layer (NBL). This apparent correlation is based upon the photochemical reaction pathway to produce both compounds. The actual formation schemes are quite different. Both compounds require RO_2 radicals in their formation processes. However, in the case of PAN, RO_2 must be the peroxyacetyl radical. Ozone formation is based on the photodissociation of NO_2 to produce NO and the O radical which reacts with oxygen to produce O_3. Likewise, NO is quickly converted to NO_2 via reaction with HO_2 or any RO_2 species, and may once again photodissociate to produce NO and O and repeat the process (reactions r1–r3, Table 1). On the other hand, the formation of PAN is chain terminating via the removal of both the peroxyacetyl radical and NO_2 from the reaction system (reaction r7). Thus, the formation pathways for O_3 are more abundant and continue as long as RO_2 species and NO_x are present, while PAN formation can more quickly deplete its precursors. Consequently, one would expect ozone production without PAN formation to occur if precursors to the peroxyacetyl radical are not present. In an atmosphere depleted of NO_2, neither compound would be produced.

Unlike O_3, PAN can form during nighttime periods by alkene ozonolysis in the presence of NO_2.[21]

H_2O_2, like PAN, is a photochemical oxidant that is formed from the oxidation of hydrocarbons in the atmosphere. The formation of H_2O_2 is primarily via the self-reaction of the HO_2 radical[21] under low NO_x conditions (Reaction r9). The predominant pathways for the formation of the hydroperoxy radical are the photolysis of formaldehyde and the oxidation of carbon monoxide (CO). Typically, H_2O_2 formation lags behind both PAN and O_3 formation in the photooxidation process. After sufficient NO_x has been consumed, NO concentrations are low and dependent upon the photostationary-state equilibrium with NO_2 and O_3. HO_2 radicals will then combine to produce H_2O_2.[22]

Diurnal profiles of PAN, H_2O_2, and O_3 (Fig. 2) behave in a manner consistent with their relationships to ambient NO_x. PAN accumulation leads H_2O_2 by 1–4 h. As PAN formation and other processes reduce the ambient levels of NO_x, H_2O_2 is able to accumulate. Of particular interest is the behavior of PAN and H_2O_2 on June 25. This day represents both the highest accumulation rate and the highest absolute maximum of PAN concentration during the entire measurement period. At 1100 EST, however, the formation of PAN seems to be dramatically cut off while O_3 and H_2O_2 production continue robustly. The continued accumulation of O_3 and H_2O_2 rules out the cessation of photochemical activity due to meteorological phenomena. In this case the rapid accumulation of PAN appears to have depleted the supply of peroxyacetyl radical by late morning, but apparently sufficient NO_x was consumed by PAN formation and other processes to create favorable conditions for H_2O_2 accumulation. In the same time period, ambient temperatures have increased, enhancing the thermal dissociation of PAN. The result is an inverse relationship between PAN and H_2O_2 on this particular day.

Diurnal Variations of O_3 and Nitrogen Species

Figure 3 illustrates the composite diurnal profiles of nitrogen species and O_3 for the entire measurement period. Total NO_y and NO_2 show consistent maxima in the early morning hours between 0600 and 0900 EST, with the average time of morning maximum being 0700 EST. (This time is calculated by noting the hour of maximum NO_2 and NO_y for each of the 33 days during the measurement period and averaging the times of maxima. This approach gives a more accurate idea of the time of maximum NO_2 and NO_y than simply reading

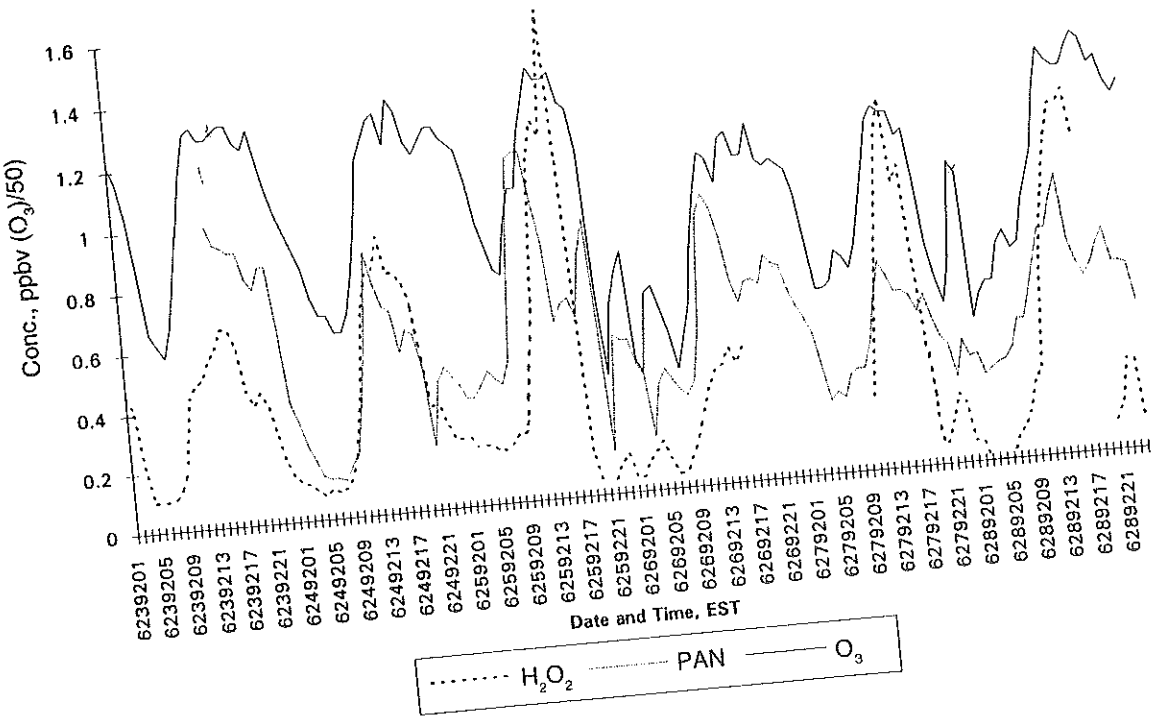

Fig. 2. Diurnal profiles of ozone, PAN, and H_2O_2 from 23 to 28 June 1992.

the time of maximum concentration from the composite average diurnal profile, because it is not influenced by the fluctuating magnitude of the maximum concentration.) The mechanism most likely to be responsible for the morning peaks of NO_2 and NO_y is regional transport of polluted airmasses above the NBL. At sunrise, when increased solar insolation triggers the breakup of the low NBL, a period of downward mixing brings the relatively undepleted polluted airmass aloft to the surface.[23] Kim et al.[8] have also suggested the possibility of enhanced biogenic emissions of NO_x from the soils during morning as contributing to morning ambient peak of NO_2 and NO_y.

The diurnal profile of NO_2 reached a minimum during the early afternoon when solar insolation was at its peak. The NO_2 concentration then gradually increased throughout the night until the rapid early morning rise to the daily maximum. It is not totally attributable to buildup of NO_2 during the collapse of the boundary layer, because such a mechanism is expected to cause a shorter and sharper increase in the concentration rather than a steady buildup in concentration for several hours.

An alternative hypothesis for the nighttime buildup of NO_2 is that the increase is due to natural emissions of nitrogen species from the local soils. A dynamic flux chamber experiment to measure nitrogen compound flux was conducted on several different days during the measurement period.[8] The results of the experiment, however, show that while there was no appreciable nighttime flux of NO_2 from the soil which could explain the buildup of NO_2 at night, frequently there was a significant level of NO flux from the soil at night. No evidence of a buildup of NO during the night was found in the data set. It seems, then, that a chemical mechanism may be converting the NO emitted from the soil during the night into NO_2. One possible mechanism for such a conversion is the titration of O_3 by NO to give NO_2. Levels of O_3 overnight are typically near 30 ppbv and are sufficient to immediately titrate any NO from the soil to NO_2 (reaction r3). Thus, the persistence of O_3 overnight at the site may facilitate the conversion of NO to NO_2 and effectively increase the background concentration of NO_2, at the site.

In Fig. 3, NO shows a morning maximum between 0700 and 0900 EST. The time of the NO peak is sometimes the same as the NO_y and NO_2 peaks, but typically follows the NO_2 peak by one to two hours. For this reason, the existence of a morning maximum of NO concentration is considered to be the combination of three separate mechanisms. The first is the same mechanism that brings NO_2 to the site; medium range transport from one of the regional urban areas followed by downward mixing during the breakup of the nocturnal boundary layer. A second possible mechanism is the regeneration of NO from NO_2 after the onset of NO_2 photolysis in the morning. To test this second hypothesized mechanism, the regeneration of NO from NO_2, a simple calculation based on photostationary state equilibrium (PSS) between NO_2, O_3, and NO was made. After assuming that photostationary state applies early in the morning, the average 0800 EST concentration of O_3 (~30 ppbv) and NO_2 (~2 ppbv) as well as the rate constant of the reaction

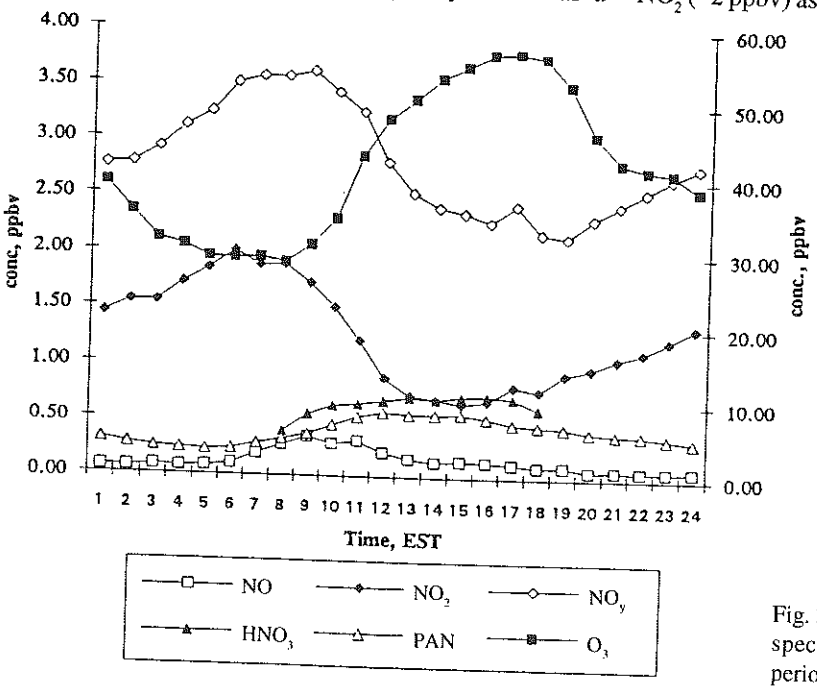

Fig. 3. Composite diurnal profiles of nitrogen species and ozone for the measurement period.

of NO with O_3, k (= 1.8×10^{-14} cm^3 molecule^{-1} s^{-1}), and J (= 4×10^{-3} s^{-1}), which is the average observed value, the photolysis rate of NO_2 are used to calculate the expected concentration of NO. The resulting concentration of NO is ~0.5 ppbv, a concentration that is comparable to that observed in the morning NO profile (Fig. 3). A third possible contributing factor responsible for a portion of the morning NO peak could be the natural injection of NO from the soil into the site environment.[8] Thus, the diurnal behavior of NO is thought to be a combination of direct transport of NO_x from regional pollution sources, the regeneration of NO by the early morning near-PSS conditions, and possibly natural emission of NO from the soil.

Gaseous HNO_3 concentrations were measured during the daytime between 0800 and 1800 EST. HNO_3 shows a typical diurnal profile with a steady increase in concentration from its morning minimum to a maximum occurring at ~1500 EST, followed by a steady decrease to nighttime lows. The diurnal profile of HNO_3 is explained by the mechanism of the daytime formation of nitric acid. HNO_3 is primarily produced through the reaction of NO_2 with OH during the daytime (reaction r6). In fact, HNO_3 typically starts to increase at the same time that NO_2 concentrations begin to decline, and the HNO_3 maximum corresponds with the NO_2 minimum in the middle of the afternoon (Fig. 3). Statistically, there was found to be a negative correlation ($[HNO_3] = -0.14[NO_2] + 0.86$, $r = -0.6$) between diurnal profiles of NO_2 and HNO_3 in our data. This correlation between NO_2 and HNO_3 is in accordance with the accepted primary pathway of the formation of HNO_3 during daytime being the reaction of NO_2 with OH at the site.

NO_x and the Ratio of NO_x/NO_y

Table 2 presents statistical summaries of the average, daytime, and nighttime concentrations of individual odd-nitrogen compounds and total NO_y measured at the site. Daytime is defined as 0700–1700 EST, and nighttime as 0200–0400 EST. All concentrations reported in this table are based on hourly averages integrated over the measurement period, except for nitric acid which is a two-hour average and was measured only during the daytime. Median concentrations of daytime NO and O_3 we found to be similar to those observed at a high elevation site (1100 m) in the Shenandoah National Park in rural Virginia, but the NO_y was about 25% higher at this site.[24] However, the NO_y concentration was found to be similar to the concentrations observed in Bondville, Illinois, and Scotia, Pennsylvania.[25] The partitioning of NO_y among individual odd-nitrogen compounds for all data are given in Table 3. The fractional contribution of each odd-nitrogen compound measured recently at several different sites in the US are also presented in Table 3.

In the absence of high deposition and dispersion the total quantity of NO_y can be conserved while the lifetime of NO_x is limited to as little as 1 day or less in the boundary layer.[26] The lifetime of NO_x depends strongly on the physical and chemical processes in the atmosphere. The obvious importance of photochemistry is in the rapid conversion of NO_x into longer lived reservoir species such as PAN and HNO_3 (reactions r6, r7). Thus the relative abundance of NO_x in the atmosphere can be used as an index of the photochemical age of the airmass.[27] An alternative expression of this photochemical age is the ratio of NO_x

Table 2. Statistical summaries of the average, daytime, and nighttime concentrations of individual odd-nitrogen compounds and total NO_y measured at site SONIA

Species	Data set	*n*	Max.	Mean	Median	S.D.
NO	day	357	1.46	0.22	0.14	0.23
	night	299	5.41	0.09	0.04	0.33
	all	785	5.41	0.15	0.07	0.29
NO_2	day	336	5.06	1.19	0.91	0.96
	night	302	7.84	1.38	1.25	0.91
	all	769	7.84	1.31	1.06	0.99
PAN	day	267	1.17	0.48	0.46	0.27
	night	216	0.86	0.33	0.32	0.17
	all	578	1.17	0.40	0.36	0.24
HNO_3	day	250	1.76	0.67	0.66	0.33
NO_y	day	333	9.31	2.97	2.78	1.49
	night	291	14.47	2.77	2.68	1.59
	all	743	14.47	2.88	2.70	1.58
Sum NO_y:	day	148	5.55	2.38	2.25	1.04

to NO_y.[28] The ratio of NO_x/NO_y reflects the degree of transformation of NO_x species to reservoir species of NO_y, but is not skewed by dilution effects or changes in the total magnitude of the concentration of nitrogen species. The NO_x/NO_y ratio is expected to be nearly unity in a freshly polluted airmass while the ratio should decrease as the airmass ages photochemically and NO_x is converted to other NO_y species. In the simplest case, where sources and sinks of NO_y are neglected, the NO_x/NO_y ratio would gradually decrease as the airmass progresses away from its anthropogenic source and ages chemically. Thus we expect a relatively high value of NO_x/NO_y in an airmass encountered a relatively short time after its exposure to anthropogenic pollution and a significantly lower value for the ratio for an airmass encountered long after its exposure to pollution. The NO_x/NO_y ratio also gives information about the nature of an airmass. For example, the ratio is found to increase from an airmass originating in a marine environment with few anthropogenic sources to a continental airmass which is more heavily impacted by anthropogenic pollution. Recent measurements show that the average NO_x/NO_y ratio in the planetary boundary layer increases from 0.14 over the ocean (Mauna Loa)[28] to as high as 0.59 over a continental rural site (Scotia, PA)[27] (Table 3).

Figure 4 shows the plots of HNO_3/NO_x vs. NO_x and PAN/NO_x vs. NO_x, respectively. Using the absolute level of NO_x as a gauge of chemical age, Fig. 4 illustrates the photochemical transformation of the active nitrogen species into the reservoir species HNO_3 and PAN. This transformation is an illustration of the airmass aging process and of local photochemical processes. There is strong correlation between the

Table 3. Partitioning of NO_y among individual odd-nitrogen compounds at site SONIA and recent results from other rural sites in the US

Species	*n*	Max.	Mean	Median	S.D.	Scotia	Niwot Ridge	Mauna Loa
NO/NO_y	568	0.38	0.05	0.03	0.05	–	–	–
NO_2/NO_y	577	1.02	0.41	0.38	0.22	–	–	–
NO_x/NO_y	568	1.40	0.45	0.41	0.27	0.59	0.32	0.14
PAN/NO_y	488	0.64	0.13	0.12	0.08	0.14	0.24	0.05
HNO_3/NO_y	180	0.64	0.21	0.19	0.11	0.16	0.13	0.43
Sum NO_{yi}/NO_y	180	–	0.80	0.72	–	0.93	0.73	0.75

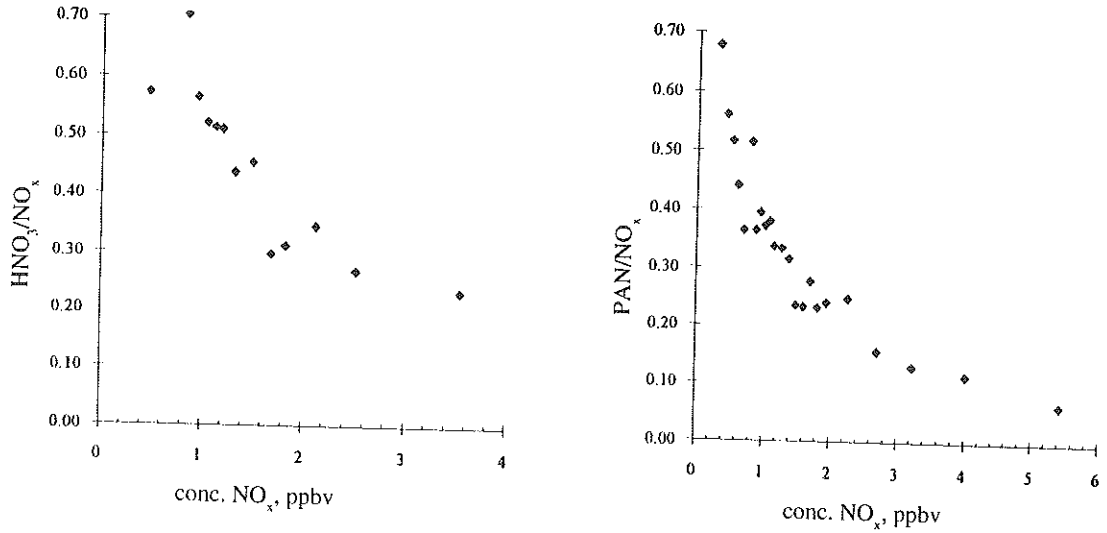

Fig. 4. Ratio of (a) HNO_3/NO_x; and (b) PAN/NO_x versus NO_x. Each cell represents (a) 10 (b) 20 data points. The cells are sorted in increasing order of NO_x concentration.

variables in each of the plots where both the HNO_3/NO_x ratio and PAN/NO_x ratio increase strongly as NO_x decreases. This relationship is expected because NO_x decreases and is converted to reservoir NO_y species as the airmass ages during transport. Also, the average diurnal profiles of NO_x, PAN, and HNO_3 clearly show that, on a local photochemical basis, both PAN and HNO_3 reach their maxima when NO_x is near its minimum at the site. These two factors of photochemical aging of a transported airmass and the impact of local photochemistry at the site combine to explain the trends shown in Fig. 4. Similar trends have been observed in the troposphere[27,29] even though the range of the ratios and NO_x levels are different because of the different nature of the experimental environment.

The NO_x/NO_y ratio ranges from 0.1 to 0.8 at site SONIA. These ratios are comparable with recent results (0.2–0.8) from two other rural sites in the United States, Niwot Ridge, Colorado, and Scotia, PA. At these sites the decline of NO_x/NO_y is also coincident with the increase in reservoir species. The range of the NO_x/NO_y ratio is 0.05 to 0.3 at Mauna Loa, Hawaii, significantly lower than at the continental sites. The lower range at Mauna Loa is not surprising in light of the much lower anthropogenic impact at the remote marine site. Also, the Mauna Loa site is at a significantly higher altitude than the continental rural sites of Scotia, PA, and Candor, NC. Hübler et al.,[30] reported median NO_y is a factor of 2–15 lower at Mauna Loa than at surface sites in the continental United States. In addition, airmasses reaching the Mauna Loa site have travelled a minimum of several days from possible anthropogenic NO_x sources. During the transport period, NO_x is converted to reservoir species and/or reactive oxidized products and suffers more loss due to wet and dry deposition.

In Fig. 5 the ratios of HNO_3/NO_y and PAN/NO_y are plotted against NO_x/NO_y. The same declining trends are evident in these plots. The ratio of PAN/NO_y and HNO_3/NO_y decreases as the ratio of NO_x/NO_y increases. The same explanation as that for Fig. 4 is used for the relationships shown in these plots. One feature to note is

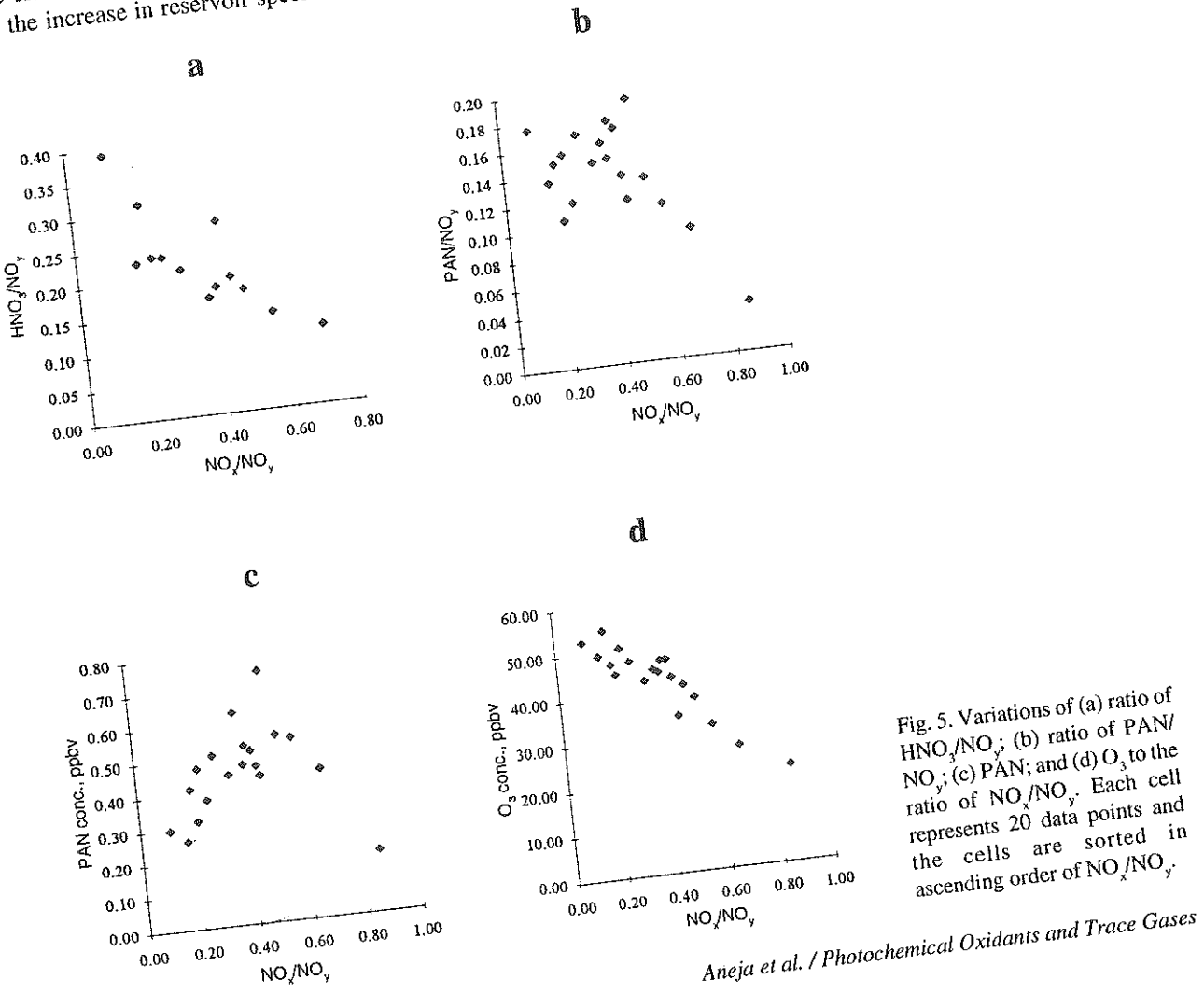

Fig. 5. Variations of (a) ratio of HNO_3/NO_y; (b) ratio of PAN/NO_y; (c) PAN; and (d) O_3 to the ratio of NO_x/NO_y. Each cell represents 20 data points and the cells are sorted in ascending order of NO_x/NO_y.

an apparent inflection point in Fig. 5b at $NO_x/NO_y \cong 0.4$. In this figure PAN as a fraction of NO_y steadily increases, as NO_x as a fraction of NO_y decreases. The trend appears to reverse at a NO_x/NO_y value of 0.4. One possible explanation for this apparent inflection point is that in the warm southeastern climate as an airmass ages, there is a continuing loss of peroxyacetyl radical due to thermal dissociation of PAN and subsequent reactions of the peroxyacetyl radical with available NO (reaction r8). NO_2, however, is regenerated and free to convert to some other NO_y species such as HNO_3. Thus, as the airmass ages, peroxyacetyl radical is continuously lost and eventually the PAN loss rate overtakes the PAN formation rate. Under the conditions encountered at site SONIA this point appears to occur where $NO_x/NO_y \cong 0.4$.

Plots of PAN and O_3 concentrations against the NO_x/NO_y ratio are shown in Fig. 5c,d. Again, PAN increases in concentration strongly as the NO_x/NO_y ratio decreases to an inflection point between 0.40 and 0.50. Thereafter, PAN concentration decreases linearly with the NO_x/NO_y ratio. In contrast, O_3 concentration increases linearly with decreasing NO_x/NO_y throughout the entire range of NO_x/NO_y. The relationship of O_3 to NO_x/NO_y is quite similar to the relationship between HNO_3/NO_y and NO_x/NO_y (Fig. 5a). O_3 is formed from photolysis of NO_2 (reactions r1, r2) when organic peroxy radicals interrupt the photostationary state. As the ratio of NO_x/NO_y decreases, a portion of that decrease can be attributed to the formation of organic nitrate compounds, particularly PAN. O_3 continues to increase with decreasing NO_x/NO_y, however, while PAN at some point will begin to decrease with decreasing NO_x/NO_y, because O_3 requires only the RO_2 radical to continue forming while PAN requires specifically the peroxyacetyl radical which is continuously lost due to reasons stated above. The relationship of both PAN and O_3 to NO_x/NO_y may also be explained by an examination of the local photochemical and transport processes. The NO_x/NO_y ratio is typically at its maximum early in the morning when NO_x is mixed downward at the breakup of the NBL. At this time, PAN and O_3 concentrations are typically near their minimum. In addition, peaks of transported O_3 and PAN rarely arrive with the NO_x peaks in the morning, and when transport does occur simultaneously between NO_x, PAN, and O_3, the magnitude of the transported PAN and O_3 is significantly smaller than that of NO_x. Thus it appears that PAN and O_3 form mostly as a result of photochemical reactions involving transported and perhaps locally generated precursor species.

As stated above, for a given airmass the NO_x/NO_y ratio provides a relative measure of the extent of photochemical interconversion between NO_x and the balance of the NO_y reservoir. The ratio therefore is expected to have a diurnal profile that corresponds with the driving force behind photochemical activity, and solar radiation. To remove any bias from the magnitude of the concentrations of the nitrogen species, the difference between NO_y and NO_x can be normalized by NO_x, i.e., $(NO_y - NO_x)/NO_x$. Figure 6 shows the diurnal variation in the $(NO_y - NO_x)/NO_x$ ratio at site SONIA. The ratio reaches a maximum value at midday when local photochemical activity reaches its peak. The observed range of the ratio at site SONIA is 1 to 4, a range that compares favorably with the results from Niwot Ridge in Colorado.[31] The average NO_x/NO_y ratio for each hour in the diurnal cycle was typically ~13% higher at site SONIA than at Niwot Ridge. The discrepancy is probably due to the lesser impact of anthropogenic sources on a regular basis because of the high altitude of the Niwot Ridge site. Niwot Ridge is frequently impacted by free tropospheric airmasses which are less affected by anthropogenic sources of NO_x. Figure 7 shows a plot of O_3 against $(NO_y - NO_x)/NO_y$. This plot shows the strength of the relationship between O_3 and the reservoir species of NO_y; i.e., the slope of the plot may indicate the degree of the O_3 formation from NO_x before the NO_x converts to NO_y in the airmass. As expected, O_3 increases as the degree of photochemical conversion of NO_x to reservoir NO_y species increases. A linear regression of O_3 and $(NO_y - NO_x)/NO_y$ is $[O_3] = 25.8 \times (NO_y - NO_x)/NO_y + 27$, $r = 0.76$. O_3 concentration is expected to be low in young airmasses because in the troposphere O_3 is mainly formed by the same photochemical processes that lead to the conversion of NO_x into reservoir species such as PAN and HNO_3. Thus, as the ratio increases, indicating a more aged airmass and more complete photo-chemical conversion of NO_x to reservoir species of NO_y, the concentration of O_3 also increases. In fact, it is expected that the ratio of O_3 to reservoir NO_y should increase as airmass age increases because of the relatively longer lifetime of O_3 than that of reservoir NO_y species such as HNO_3 and PAN. In a very old airmass with the value of the $(NO_y - NO_x)/NO_y$ ratio approaching unity, the O_3 should continue to increase, while the reservoir NO_y species begin to decrease due to their shorter lifetimes. This hypothesis leads one to expect the slope of O_3 vs. the $(NO_y - NO_x)/NO_y$ ratio to steepen as the value of the ratio approaches unity. Indeed, Fig. 7 seems to confirm this hypothesis with a nearly flat slope in the 0.0 to 0.5 range, and a sharply steeper slope in the 0.5 to 1.0 range. The relationship is similar to that seen in the PAN vs. NO_x/NO_y plot, suggesting that there is some age at which reservoir species begin to become depleted, while O_3 continues to build.

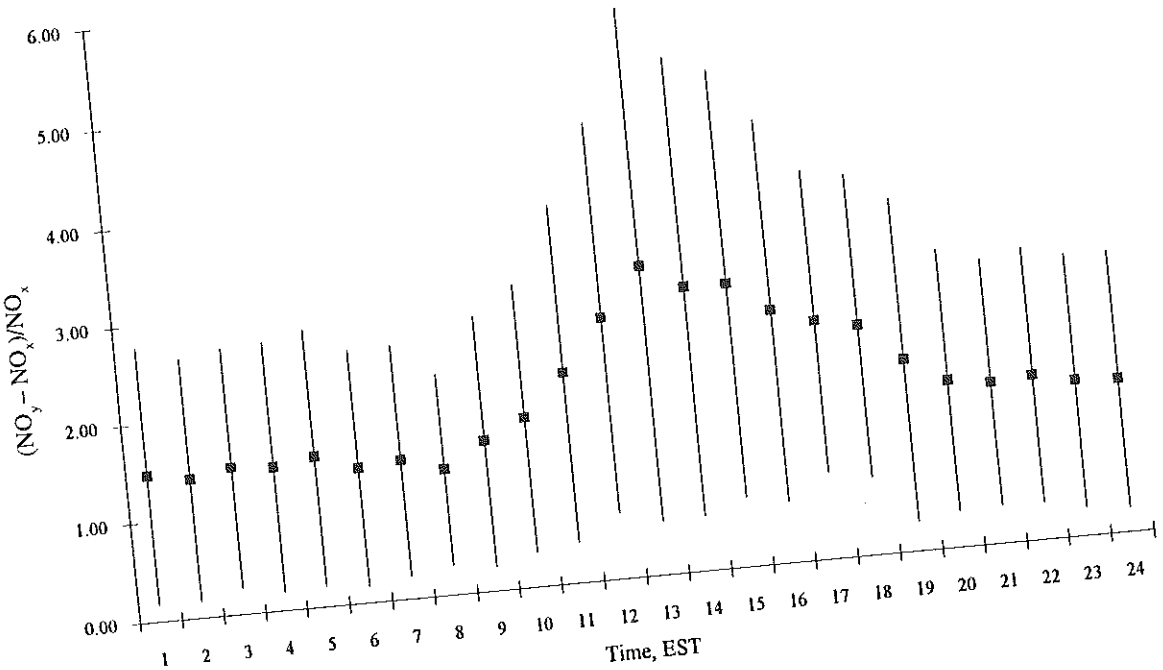

Fig. 6. Composite diurnal profile of NO_x photochemical product formation $[(NO_y - NO_x)/NO_x]$ for the measurement period.

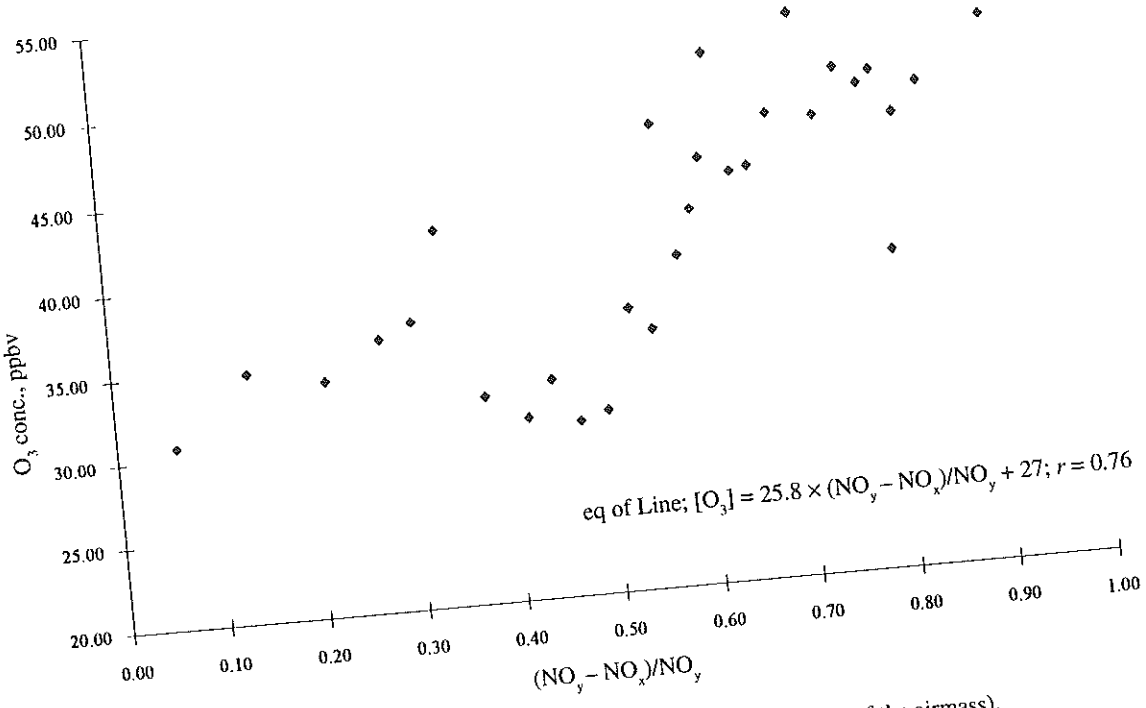

Fig. 7. Variation of O_3 versus the ratio of $(NO_y - NO_x)/NO_y$ (i.e., photochemical aging of the airmass).

The regression equation of O_3 and $(NO_y - NO_x)/(NO_y)$ given above can be rewritten as $O_3 = 25.8/NO(NO_y - NO_x) + 27$. Substituting the average value for NO_y (2.92), the equation then reduces to $O_3 = 8.84 (NO_y - NO_x) + 27$. From this equation, it is seen that the background ozone concentration at this rural site is about 27 ppbv, which is typical of the eastern US background ozone concentration.[23] The value of 8.8 for the slope of the line $[NO_y - NO_x]$ vs. $[O_3]$ can be interpreted as the number of O_3 molecules formed for every NO_x molecule oxidized to its oxidative products, which is similar to the value of 8.5 reported by Trainer et al.[32]

Photostationary State (PSS) Constant and O_3 Formation

In an atmosphere containing only NO_x and air (no organics), the reactions which determine the concentration of NO and NO_2 and the formation of O_3 are reactions r1, r2, and r3 in Table 1. When the time rate of change of O_3 is defined as zero, this relationship is known as the photostationary state. The PSS assumption leads to an expression of $[O_3]$, $[NO_2]$, [NO], J, and k_3, the Leighton relationship,

$$\frac{[O_3][NO]}{NO_2} = \frac{J}{k_3}$$

where J and k_3 are the rate constants for the photolysis of NO_2 and for the reaction of NO with O_3 (reaction r3), respectively. According to this relationship, the ratio of $[O_3]$, [NO], and $[NO_2]$ at any time in an airmass should be a constant given by the ratio of J and k_3. Thus, the quantity J/k_3 should exhibit a diurnal profile because the value of J varies (1×10^{-3} to ~9×10^{-3} s^{-1})[33] with the inclination of the sun and with the sky condition over the site, and k_3 (= 1.8×10^{-14} cm^3 $molecules^{-1}$ s^{-1} at 298 K)[21] varies with temperature.

PSS equations have been used in the past to estimate the O_3 formation rate at different locations in the US.[3,34–38] The PSS constant obtained from the values of $[O_3]$, [NO], and $[NO_2]$ measured at the site is used in this section to examine the relationship between the accumulation rate of O_3 and the deviation from the photostationary state.

Figure 8 shows the diurnal variation of the value of $[O_3][NO]/[NO_2]$ for each hourly observation, and PSS constant (J^*/k_3) estimated from J values scaled by hourly averaged solar radiation measured at the site and k_3, shown as a solid line. The dotted line denotes the average value of the ratio (hereafter referred to as the measured PSS constant). Figure 8 illustrates that approximately 70% of the measured PSS constants were below estimated PSS constant (J^*/k_3) for the hour,

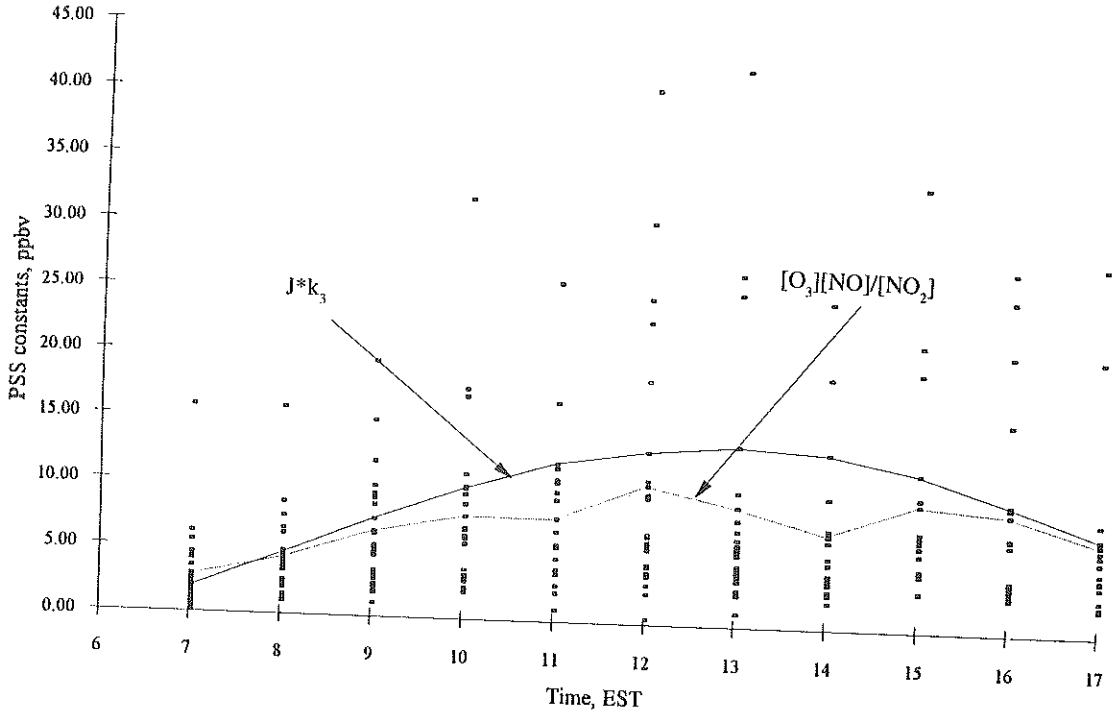

Fig. 8. Diurnal variations of photostationary state (PSS) constants based on the ratio of hourly averaged O_3, NO, and NO_2 concentrations and calculated PSS constant (J^*/k_3).

implying that the photostationary state is routinely disturbed at the site. These results suggest that O_3 is accumulating at the site from local photochemical activity involving precursors, i.e., NO_x and VOCs, which may either be transported and anthropogenic in origin or local biogenic precursors. The role of transport in the O_3 concentrations found at the site should not be ignored, particularly in light of the clear evidence of regional transport of NO_x to our site. It is noted, however, that O_3 peaks were rarely observed to be coincident with NO_x transport episodes. An increased abundance of peroxy radicals in ambient air is responsible for the disturbance of the photostationary state because of their preferential competition (reactions r4, r5) with O_3 for NO.

In order to determine a mathematical relationship for the accumulation of O_3 in the non-photostationary state, reactions r4 and r5 must be considered in conjunction with reactions r1–r3. The concentrations of NO_2 and NO may still be assumed to be at steady state, as the net result of reactions r3–r5 is conversion of NO to NO_2. However, the relative importance of the three pathways for the reaction of NO depends on the level of reactants available and the magnitude of the rate constants for each reaction. The rate of change of the concentration of O_3 in this non-photostationary state situation may be calculated from the following first-order differential equation if no other sources or sinks for O_3 are allowed:

$$\frac{d[O_3]}{dt} + k_3[NO][O_3] = J[NO_2] \qquad (1)$$

The solution for this equation for $[O_3]$ at time t is as follows:

$$[O_3]_t = [1 - (1 - \frac{k_3[NO]}{J[NO_2]}\ [O_3]_0)\ e^{-k_3[NO]t}) / \frac{k_3[NO]}{J[NO_2]} \qquad (2)$$

where $[O_3]_0$ is the initial O_3 concentration. If initial $[O_3]$ is zero, eq 2 may be written as:

$$[O_3]_t = (1 - e^{-k_3[NO]t}) / \frac{k_3[NO]}{J[NO_2]} \qquad (3)$$

This solution shows that O_3 concentration increases with time and that the rate of the increase depends on the ratio of the loss reaction of O_3 to the photolysis of NO_2. Finally, the ratio of the concentrations of [NO], $[NO_2]$, and $[O_3]$ approaches the quantity J/k_3 as time approaches infinity, or expressed in another way, as time approaches infinity the system approaches the photostationary state. This relationship is understandable from the standpoint that as the peroxy radicals are used up in their reaction with NO, they are removed from the system. The system then returns to the photostationary state. Thus, the O_3 maximum occurs when the system reaches the PSS. The O_3 concentration calculated under PSS conditions may thus be considered an upper bound for O_3-forming potential from a given NO_x balance.

Diurnal variation of O_3 (Fig. 3) may be explained by considering the change in solar intensity throughout the day and the implications of that change on the PSS. O_3 concentration starts to increase at 0800 EST and reaches its maximum around 1600 EST. The average range of O_3 concentrations is 30–60 ppbv. Photochemistry is initiated in the morning, and O_3 is accumulated because the peroxy radicals formed from local biogenic hydrocarbons and, possibly, transported hydrocarbons interrupt the loss reaction of O_3 with NO. The atmosphere is expected to reach its maximum deviation from the photostationary state situation as solar radiation reaches its maximum (Fig. 8). The time rate of change of the concentration of O_3 is also expected to reach its maximum at the time of maximum deviation from PSS. The system is then expected to return to PSS balance as solar intensity diminishes after around 1700 EST (Fig. 8). Consequently, the magnitude of the time rate of change of O_3 is dependent on the ambient level of peroxy radicals which drive down the efficiency of the loss rate of O_3 with NO. Additionally, the maximum potential level of $[O_3]$ may be sensitive both to the [NO]/$[NO_2]$ ratio and to the NO_2 photolysis rate constant, J.

SUMMARY AND CONCLUSIONS

As part of the SOS project, we conducted an intensive field experiment at a rural site, site SONIA in the central Piedmont region of North Carolina, USA. In order to establish the background concentrations of different chemical species at this rural site, i.e., photochemical oxidants (O_3, PAN, and H_2O_2), various trace gas species including reactive odd-nitrogen compounds as well as total NO_y were measured. The diurnal variations of the photochemical oxidants were investigated as a sum of their formation and removal processes. The diurnal variation of each NO_y species was also discussed and the relationship between NO_x and total NO_y was explored on the basis of airmass origin and age. The relationship between NO_x and NO_y was also used to determine the extent of chemical processing among the nitrogen species in an airmass and the relationship of that chemical processing to photochemical oxidants (O_3, HNO_3, and PAN).

The mean NO_y concentration was found to be 2.63 ppbv (median 2.57 ppbv). The mean concentrations of NO, NO_2, HNO_3, PAN, and H_2O_2 were found to be 0.18, 1.31, 0.67, 0.41, and 0.52 ppbv, respectively. Each species showed diurnal variations (Figs. 2, 3). NO_y, NO, and NO_2 maxima occurred in the morning between 0500 and 0900 EST. The NO_y and NO_2 maxima typically

occurred around 0700 EST. It is likely that the NO_x mixed down to the surface during the morning breakup of the NBL. The NO peak at the site could also be supplied by downward mixing of polluted airmasses, but the short lifetime of NO and the lack of strong correlation between the NO_2 and NO peaks suggests other mechanisms may be at work. Possible other mechanisms responsible for the NO peaks at 0900 EST are conversion of NO_2 to NO by photolysis and peroxy radicals available at the time in the morning or natural NO flux from the soil. A soil flux experiment conducted over the measurement period showed elevated morning flux of NO in 30% of the samples, suggesting enhanced emissions of NO from soils as a possible source. PAN, HNO_3, H_2O_2, and O_3 diurnal variation were quite similar, suggesting they might share a common source, probably mesoscale photochemical production from transported and locally produced precursor species.

The NO_x/NO_y ratio, as well as the quantity $(NO_y - NO_x)/NO_y$ were used as "chemical clocks" of an airmass, and the photochemical oxidants were correlated with these measures of airmass age (Figs. 5, 7). From a linear regression of O_3 on $(NO_y - NO_x)/NO_y$, it was found that ~9 molecules of O_3 were produced for every NO_x molecule oxidized to its oxidative products. Background concentration of O_3 at this rural site was found to be ~27 ppbv. Both O_3 and HNO_3 concentrations increased linearly with increasing chemical airmass age. However, the relationship between PAN concentration and the NO_x/NO_y ratio revealed that PAN increased to an inflection point between 0.40 and 0.50. Thereafter, PAN concentration decreased linearly with the NO_x/NO_y ratio. It seems that the levels of the photochemical oxidants O_3, HNO_3, and PAN are heavily impacted by the concentration of NO_x and the NO_x/NO_y ratio.

The relationship between the accumulation rate of O_3 and deviation from the photostationary state was examined based on a measured PSS constant obtained from the values of $[O_3]$, [NO], and $[NO_2]$ measured at the site (Fig. 8). The rate of O_3 accumulation was found to be correlated with the deviation of the measured PSS constant from the PSS constant calculated from J^*/k_3. Comparison of the measured and calculated PSS constant illustrates the diurnal deviation of the local photochemical environment from the photostationary state. The maximum deviation from the photostationary state is found during mid-afternoon, suggesting that the O_3 accumulation rate may be maximum during these hours.

In conclusion, while this study has shed some light on the behavior of oxidants in the Southeast US, it is clear that more comprehensive research into the role of naturally produced nitrogen species and their characteristics is needed to enhance our understanding of the photochemical processes leading to their production there. The understanding gained from this field research and the photochemical models developed are of great importance to the formation of basic pollution control strategy in the Southeast US.

Acknowledgments. This research has been funded by the US Environmental Protection Agency through a cooperative agreement with the University Corporation for Atmospheric Research (S 9192) as part of the Southern Oxidants Study–The Southern Regional Oxidant Network (SOS–SERON). We acknowledge Dr. W. Lonneman, US EPA, for assisting us in the PAN measurements; Mr. G. Murray, N.C. DENHR for systems audit; Dr. H. Jeffries, University of North Carolina at Chapel Hill, Dr. B. Gay, US EPA, Dr. M. Rodgers, Georgia Institute of Technology, and members of our Air Quality group, Zheng Li, and Eric Ringler for their assistance and discussions on atmospheric oxidants; Ms. M. DeFeo and Ms. B. Batts for the preparation of the manuscript.

Disclaimer. The contents of this document do not necessarily reflect the views and policies of the US Environmental Protection Agency, the University Corporation for Atmospheric Research, nor the views of all members of the Southern Oxidants Study Consortia, nor does mention of trade names or commercial or noncommercial products constitute endorsement or recommendation for use.

REFERENCES

(1) National Research Council Committee on Tropospheric Ozone Formation and Measurement. Rethinking the Ozone Problem in Urban and Regional Air Pollution; National Academy Press: Washington, DC, 1991, 500 pp.
(2) Lindsay, R.W.; Richardson, J.L.; Chameides, W.L. *J. Air Pollut. Control Assoc.* 1989, **39**: 40–43.
(3) (a) Ridley, B.A.; Madronich, S.; Chatefield, R.B.; Walega, J.G.; Shetter, R.E.; Carroll, M.A.; Montzka, D.D. *J. Geophys. Res.* 1992, **97**: 10,375–10,388. (b) Ridley, B. A.; Robinson, E. *J. Geophys. Res.* 1992, **97**: 10285–10290.
(4) Logan, J. A. *J. Geophys. Res.* 1983, **88**: 10785–10807.
(5) Slemr, F.; Seiler, W. *J. Atmos. Chem.* 1984, **2**: 1–24.
(6) Williams, E. J.; Parrish, D.D.; Fehsenfeld, F.C. *J. Geophys. Res.* 1987, **92**: 2173–23179.
(7) Johansson, C.; Sanhueza E. *J. Geophys. Res.* 1980, **93**: 14193–14198.
(8) Kim, D.S.; Aneja, V.P.; Robarge, W.P. *Atmos. Environ.* 1994, **28**: 1129–1137.
(9) Aneja, V.P.; Robarge, W.P.; Holbrook, B.D. *Atmos. Environ.*, in press.
(10) Williams, E.J.; Guenther, A.; Fehsenfeld, F.C. *J. Geophys. Res.* 1992, **97**: 7511–7519.
(11) Crutzen, P.J. *Annu. Rev. Earth Planet. Sci.* 1979, **7**: 443–472.
(12) (a) Singh, H. B.; Hanst, P.L. *Geophys. Res. Lett.* 1981,

8: 941. (b) Singh, H. B.; Salas, L.J. *Atmos. Environ.* 1989, **23**: 231–238.
(13) Meagher, J.F.; Lee, N.T.; Valente, R.J.; Parkhurt, W.J. *Atmos. Environ.* 1987, **21**: 605–615.
(14) Aneja, V.P.; Claiborn, C.S.; Li, Z.; Murthy, A. *J. Air Pollut. Waste Manage. Assoc.* 1990, **40**: 217–220.
(15) Kleinman, L; Lee, Y.–N.; Springston, S.R.; Nunnermacker, L.; Zhou, X.; Brown, R.; Hallock, K.; Klotz, P.; Leahy, D.; Lee, J.H.; Newman, L. *J. Geophys. Res.* 1994, **99**: 3469–3482.
(16) Delany, A. C.; Dickerson R.R.; Melchior F.L.Jr.; Wartburg, A.F. *Rev. Sci. Instrum.* 1982, **53**: 1899–1902.
(17) Dickerson, R. R.; Delany, A.C.; Wartburg, A.F. *Rev. Sci. Instrum.* 1984, **55**: 1995–1998.
(18) LMA–3 LUMINOX Operation Manual, SCINTREX/ UNISEARCH, Concord, Ontario, Canada, 1987.
(19) Lazrus, A.L.; Kok, G.L.; Lind, J.A.; Gitlin, S.N.; Heikes, B.G.; Shettes, R.E. *Anal. Chem.* 1986, **58**: 594–597.
(20) Healey, J. "The Quality Assurance Plan for the Southern Oxidants Research Program on Ozone Non–Attainment," Revision 1, 1991: The Fleming Group, Albany, NY.
(21) Finlayson–Pitts, B.J.; Pitts J.N.Jr. *Atmospheric Chemistry: Fundamentals and Experimental Techniques*; Wiley: New York, 1986, pp. 526–528.
(22) Dollard, G.J.; Jones, B.M.R.; Davies, T.J. *Atmos. Environ.* 1991, **25A**: 2039–2053.
(23) Trainer, M.; Williams, E.J.; Parrish, D.D.; Buhr, M.P.; Allwine, E.J.; Westberg, H.H.; Fehsenfeld, F.C.; Liu, S.C. *Nature* 1987, **329**: 705–707.
(24) Doddridge, B.G.; Dickerson, R.R.; Wardell, R.G.; Civerolo, K.L.; Nunnermacker, L.J. *J. Geophys. Res.* 1992, **97**: 20,631–20,646.
(25) Parrish, D.D.; Trainer, M.; Buhr, M.P.; Watkins, B.A.; Fehsenfeld, F.C. *J. Geophys. Res.* 1993, **98**: 2927–2940.
(26) Spicer, C.W. In *Advances in Environmental Science and Technology*; Pitts, J.N.,Jr.; Metcalf, R.L., Eds.; Wiley: New York, 1977; Vol. 7, pp. 182–197.
(27) Ridley, B.A. *Atmos. Environ.* 1991, **21**: 569–578.
(28) Atlas, E. L.; Ridley, B.A.; Hubler, G.; Walega, J.G.; Carroll, M.A.; Montzka, D.D.; Huebert, B.J.; Norton, R.B.; Grahek, F.E.; Schauffler, S. *J. Geophys. Res.* 1992, **97**: 10,449–10,462.
(29) Huebert, B.J., et al. *J. Geophys. Res.* 1990, **95**: 10,193–10,198.
(30) Hubler, G.; Fahey, D.; Ridley, B.A.; Gregory, G.L.: Fehsenfeld, F.C. *J. Geophys. Res.* 1992, **97**: 9833–9850.
(31) Fahey, D. W.; Hubler, G.; Parrish, D.D.; Williams, E.J.; Norton, R.B.; Ridley, B.A.; Singh, H.B.; Liu, S.C.; Fehsenfeld, F.C. *J. Geophys. Res.* 1986, **91**: 9781–9793.
(32) Trainer et al. *J. Geophys. Res.* 1993, **98**: 2917–2925.
(33) Madronich, S. Intercomparison of NO_2 photodissociation and U.V. Radiometer Environmental Management/ Air Quality Section. 1989 Ambient Air Quality Report, May 1991.
(34) Parrish, D.D.; Trainer, M.; Williams, E.J.; Fahey, D.W.; Hübler, G.; Eubank, C.S.; Liu, S.C.; Murphy, P.C.; Albritton, D.L.; Fehsenfeld, F.C. *J. Geophys. Res.* 1986, **91**: 5361–5370.
(35) Chameides, W.L.; Davies, D.D.; Bradshaw, J.; Sandholm, S.; Rodgers, M.; Baum, B.; Ridley, B.; Madronich, S.; Carroll, M.A.; Gregory, G.; Schiff, H.I.; Hastie, D.R.; Torres, A.; Condon, E. *J. Geophys. Res.* 1990, **95**: 10,235–10,247.
(36) Davis, D.D.; Chen, G.; Chameides, W.; Bradshaw, J.; Sandholm, S.; Rodgers, M.; Schendal, J.; Madronich, S.; Sachse, G.; Gregory, G.; Anderson, B.; Barrick, J.; Shipham, M.; Collins, J.; Wade, L.; Blake, D. *J. Geophys. Res.* 1993, **98**: 23,501–23,523.
(37) Cantrell, C.A. Lind, J.A.; Shetter, R.E.; Calvert, J.G.; Goldan, P.D.; Kuster, W.; Fehsenfeld, F.C.; Montzka, S.A.; Parrish, D.D.; Williams, E.J.; Buhr, M.P.; Westberg, H.H.; Allwine, G.; Martin, R. *J. Geophys. Res.* 1992, **97**: 20,671–20,686.
(38) Poulida, O.; Civerolo, K.L.; Dickerson, R.R. *J. Geophys. Res.* 1994, **99**: 10,553–10,563.